

Critical Droplet Theory Explains the Glass Formability of Aqueous Solutions

Matthew Warkentin,^{*} James P. Sethna, and Robert E. Thorne^{*}

Physics Department, Cornell University, Ithaca, New York 14853, USA

(Received 25 September 2012; published 3 January 2013)

When pure water is cooled at $\sim 10^6$ K/s, it forms an amorphous solid (glass) instead of the more familiar crystalline phase. The presence of solutes can reduce this required (or “critical”) cooling rate by orders of magnitude. Here, we present critical cooling rates for a variety of solutes as a function of concentration and a theoretical framework for understanding these rates. For all solutes tested, the critical cooling rate is an exponential function of concentration. The exponential’s characteristic concentration for each solute correlates with the solute’s Stokes radius. A modification of critical droplet theory relates the characteristic concentration to the solute radius and the critical nucleation radius of ice in pure water. This simple theory of ice nucleation and glass formability in aqueous solutions has consequences for general glass-forming systems, and in cryobiology, cloud physics, and climate modeling.

DOI: [10.1103/PhysRevLett.110.015703](https://doi.org/10.1103/PhysRevLett.110.015703)

PACS numbers: 64.60.Q-, 05.40.-a, 64.70.dg

Ice nucleation and growth are of major interest in fields ranging from cryobiology to atmospheric physics. Ice is a key issue in cryopreservation of cells and tissues [1] and in cryocooling of samples for macromolecular crystallography [2,3], where solutes like salts, sugars, alcohols, and polyols can have dramatic effects on ice formation. In atmospheric physics, models of cloud formation are sensitive to the nature of the critical nucleus of ice crystals [4] with implications for climate models [5]. Supercooled water is an interesting system in its own right [6], and the formation of crystalline phases from supercooled solutions is an active area of study [7].

Previous experiments have focused on properties such as the melting and glass transition temperatures, and models to explain the data have largely been phenomenological. Similar models have been applied to explain glass formability in a wide variety of nonaqueous systems. Here, we report measurements of the minimum cooling rates [or “critical cooling rates” (CCRs)] required to prevent ice formation in aqueous solutions during cooling to ~ 100 K or below. We show that a surprisingly simple statistical modification to classical thermodynamic nucleation theory provides an excellent account of these data.

We studied eight different solutes (see Fig. 1), including a salt (sodium chloride), simple alcohols (methanol, ethanol), sugars (dextrose, trehalose), polyols (glycerol, ethylene glycol), and polyethylene glycol 200 (PEG 200). All are compact and highly soluble and can have large effects on critical cooling rates required for vitrification.

The effects of these solutes on ice nucleation were evaluated by measuring the critical cooling rate above which no ice was observed. Below the critical rate, a sample turns opaque on cooling, indicating the formation of polycrystalline ice. As the rate increases, a transition to transparent samples is observed. This optical transition corresponds to a transition in the x-ray diffraction patterns obtained from the cooled samples [8]. Clear samples show diffuse rings

characteristic of a glassy state, whereas opaque samples show a sharp ring characteristic of a crystalline powder.

As described in more detail elsewhere [9], ultrathin-wall plastic tubing was filled with the solution of interest and plunged into liquid nitrogen. Cooling rates were varied by varying the tube diameter and were directly measured for a reference solution using thermocouples threaded down the tube center. For each tubing diameter, solutions with solute concentration increasing in 2% increments were sequentially cooled until the crystalline-to-amorphous transition was observed; the cooling rate in that tubing diameter was recorded as the CCR for that concentration. Cooling rates

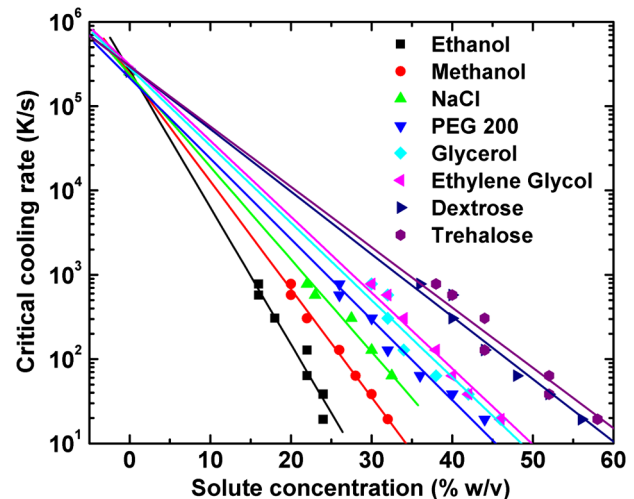


FIG. 1 (color online). Critical cooling rate (CCR)—the minimum cooling rate to obtain a vitrified sample—of aqueous solutions as a function of solute concentration, for each of the eight solutes studied. Solid lines represent exponential fits of the form $CCR = CCR_0 e^{-\beta c}$, where c is the solute concentration. The fits extrapolate to similar values of $\sim 3 \times 10^5$ K/s at $c = 0$ (corresponding to pure water).

examined here varied from ~ 10 to 1000 K/s, much larger than achieved in previous calorimetric studies, allowing CCR determination at much lower solute concentrations.

Figure 1 shows the resulting CCR versus concentration data for eight cryoprotectants, with the data for glycerol taken from Ref. [9]. Two features are noteworthy. First, for all solutes, the CCR varies exponentially with concentration over the 2 orders of magnitude in cooling rate studied. Second, each exponential extrapolates to a value between 10^5 and 10^6 K/s at zero concentration, in agreement with the estimated value for the CCR of pure water [10,11]. It is thus likely that the CCR remains exponential in concentration to zero concentration. This suggests that a simple theory, encompassing all solutes at all concentrations, can be used to explain the data.

We begin by assuming that at cooling rates near the CCR, the limiting step in ice formation is cubic ice (I_c) nucleation at a temperature near 200 K. This is justified for several reasons. First, unlike at small cooling rates, just below the CCR there is comparatively little time for nuclei to grow before the uncrystallized sample fraction vitrifies. Second, the ice nucleation rate peaks strongly near 200 K, but the growth rate there is small and decreases rapidly on further cooling [12–16]. Third, x-ray diffraction experiments suggest that the transition versus cooling rate or concentration between crystalline and amorphous samples is discontinuous [8]; if growth was limiting, one would expect a continuous transition as samples were trapped with various ensembles of growing ice clusters after cooling at different rates. Finally, it is known that the formation of a small (~ 20 Å) cubic ice cluster precedes conversion to and growth of a larger hexagonal ice cluster [4,17].

We consider cubic ice nucleation in a concentrated solution as being composed of two steps. First, local concentration fluctuations must give rise to a region of pure liquid water large enough for cubic ice to nucleate. Then, nucleation proceeds as it would in the pure system. This simplified picture allows us to write the nucleation rate for nuclei of size V as

$$J_n = J_0 P_n^V, \quad (1)$$

where J_0 is the nucleation rate in the pure system, J_n is the nucleation rate in a solution with solute number density n , and P_n^V is the probability of finding a region of volume V empty of solutes. If the solutes are ideal (i.e., they behave as an ideal gas), the number m within V will be given by a Poisson distribution with an average given by the concentration [18]. Evaluating this distribution at $m = 0$ gives

$$P_n^V = e^{-nV} \quad (2)$$

and

$$J_n = J_0 e^{-nV}. \quad (3)$$

The assumption of nucleation-dominated ice formation implies that the critical cooling rate should be proportional

to the ice nucleation rate. Consequently, it is clear that (3) can be used to describe the data in Fig. 1 with each solute having an exponential dependence of CCR on concentration n and a solute-specific characteristic volume.

To evaluate and interpret this volume, we incorporate the effect described by (3) into classical nucleation theory. For a pure system, the change in free energy on formation of a spherical ice cluster of a given radius, R_{I_c} , is

$$\Delta G_0 = -\frac{4}{3}\pi(\Delta g_v)R_{I_c}^3 + 4\pi\sigma R_{I_c}^2, \quad (4)$$

where Δg_v and σ are the bulk and surface free energy density changes, respectively, and I_c indicates cubic ice. The maximum of the function ΔG_0^* —the barrier to nucleation—occurs at the critical radius given by

$$R_{I_c}^* = \frac{2\sigma}{\Delta g_v}. \quad (5)$$

The nucleation rate can then be written as

$$J_0 = A e^{-\Delta G_0^*/k_B T}, \quad (6)$$

where A is a prefactor that will not concern us for the remainder of the discussion. The effect of a solute can be expressed by combining and (3) and (6), which gives

$$J_n = A e^{-\Delta G_0^*/k_B T} e^{-nV}.$$

This suggests a modification to the classical free energy of a cluster,

$$\Delta G_n = -\frac{4}{3}\pi(\Delta g_v)R_{I_c}^3 + 4\pi\sigma R_{I_c}^2 + \frac{4}{3}\pi n k_B T (R_{I_c} + R_s)^3, \quad (7)$$

where we assume that Δg_v and σ are the values for the pure system. The first two terms are common to (4) while the third term represents the free energy of excluding the solute

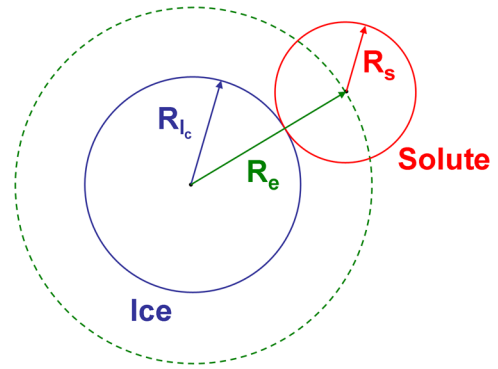


FIG. 2 (color online). Schematic illustration of the exclusion volume involved in cubic ice (I_c) nucleation. If the region inside radius R_{I_c} is to be completely free of solutes, the center of mass of all solute atoms must be excluded from a region of radius $R_e = R_{I_c} + R_s$. Differences in effective solute radii R_s are responsible for the differences in slope in Fig. 1.

TABLE I. Percent weight per volume (% w/v) to molarity conversion factors and maximum measured concentrations for each of the eight solutes in Fig. 1.

Solute	MW (g/mol)	Maximum solute concentration	
		% (w/v)	M
Ethanol	46.1	24	5.2
Methanol	32.0	32	10.0
NaCl	58.4	32	5.5
PEG 200	200	44	2.2
Glycerol	92.1	39	5.0
Ethylene glycol	62.1	46	7.4
Dextrose	180.1	56	3.1
Trehalose	342.3	58	1.7

from the spherical region of radius R_{I_c} . As shown in Fig. 2, for a solute of size R_s , this requires that the solute's center of mass be excluded from a volume of radius $R_{I_c} + R_s$. The factor $nk_B T$ in the third term of the free energy can be recognized as a microscopic osmotic pressure [19].

From (7), the energy barrier to nucleation in the presence of solutes is then

$$\Delta G_n^* = \Delta G_0^* + \frac{4}{3}\pi nk_B T (R_{I_c}^* + R_s)^3 + O(nk_B T / \Delta g_v)^2, \quad (8)$$

where $R_{I_c}^*$ is the critical nucleation radius for cubic ice in pure water. The size of the expansion parameter $nk_B T / \Delta g_v$ can be estimated from $\Delta g_v = \Delta h_v - T \Delta s_v \approx L(\Delta T / T_m)$ where L is the latent heat of fusion, T_m is the melting temperature, and ΔT is the undercooling at which nucleation occurs. Using $L = 334$ J/kg and $T_m = 273$ K for hexagonal ice and $\Delta T = 73$ K gives $nk_B T / \Delta g_v = 0.18$ for n corresponding to a 10 M solution. As shown in Table I, the maximum concentrations in Fig. 1 of all solutes except methanol are smaller than this value.

Assuming that the CCR is proportional to nucleation rate, (8) yields

$$CCR_n = CCR_0 e^{-V_e n}, \quad V_e = 4/3\pi(R_{I_c}^* + R_s)^3. \quad (9)$$

This implies that the slope of the data for each solute in Fig. 1 is set by the volume V_e of the sphere from which the solute's center of mass must be excluded; the radius of this sphere is the sum of the radius of a critical nucleus in the pure system and the solute's radius.

Figure 3 shows the ‘‘exclusion radius’’ $R_e = R_{I_c}^* + R_s$ obtained from the fits in Fig. 1 for each solute versus its Stokes radius [calculated from measured self-diffusion constants at $T = 298$ K (Table II)]. The solid line is $R_e = R_{I_c}^* + R_{\text{Stokes}}$ with $R_{I_c}^* = 7.5$ Å, based on Huang and Bartell's value $R_{I_c}^* = 7.3$ – 7.8 Å [13] derived by modeling the time evolution of electron diffraction patterns from freezing water clusters. Previous studies found that the

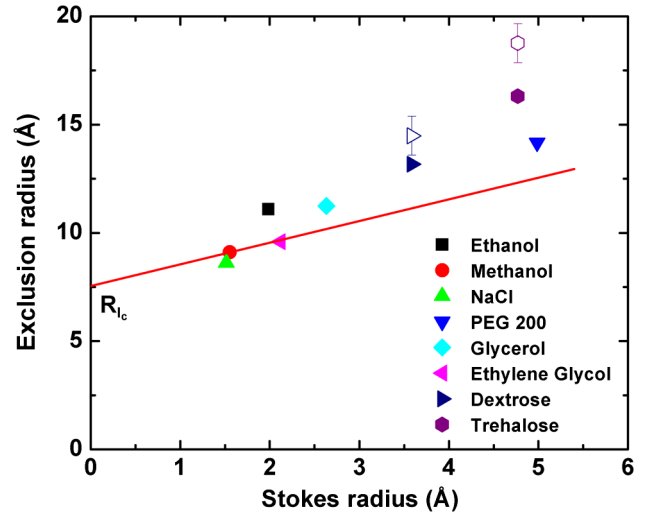


FIG. 3 (color online). The exclusion radius R_e determined for each solute versus the solute's Stokes radius. The solid line is the model prediction: $R_e = R_{I_c}^* + R_{\text{Stokes}}$ with a critical radius for pure water $R_{I_c}^* = 7.5$ Å [13]. The open symbols are calculated as $R_e = R_{I_c}^* + R_{\text{Stokes}} + R_H$, where R_H is the hydration shell thickness measured by THz spectroscopy in Ref. [23].

self-diffusion constants of many different solutes correlate with their ability to increase supercooling capacity [21]. This is reasonable because the Stokes radius relates to the microscopic dynamics of the hydrated solute at the molecular scale on which ice nuclei form.

The prediction in Fig. 3 underestimates the exclusion radius R_e for solutes with larger Stokes radii. This may result because the dynamical hydration shell relevant in solvent nucleation may be thicker than that relevant in the relatively slow dynamics that dominate solute diffusion and the Stokes radius [22]. For example, glucose and trehalose have Stokes radii of 3.5 and 4.7 Å, respectively. When probed on the picosecond time scale [23], corresponding to that for rearrangements of the hydrogen bonding network [24] that might be expected to impact nucleation, their hydration shell thicknesses are 3.7 and 6.5 Å, respectively.

TABLE II. Measured self-diffusion coefficients and calculated Stokes radii for the solutes studied. All measurements were at 298 K.

Solute	Self-diffusion constant (10^{-10} m ² s ⁻¹)	Stokes radius (Å)	Reference
Ethanol	12.2	1.99	[20]
Methanol	15.6	1.55	[20]
Sodium chloride	16.0	1.52	[21]
PEG 200	4.86	4.99	[21]
Glycerol	9.21	2.63	[21]
Ethylene glycol	11.4	2.13	[21]
Dextrose	6.75	3.59	[21]
Trehalose	5.08	4.77	[21]

The sum of these hydration shell radii and the corresponding Stokes radii (which include a contribution from hydration [22]) is indicated by the open symbols in Fig. 3.

The dynamical hydration shell and its effects on ice nucleation are known in other contexts. Computational studies show that there is a ~ 5.5 Å shell of water with altered structure and altered rotational and translational dynamics on the picosecond time scale surrounding carbohydrates [25]. IR spectroscopy of water dynamics in nanometer-size reverse micelles show that approximately half of the water in a 4 nm diameter micelle is “interfacial” while the other half is bulk-like [26], implying a 5.6 Å interfacial layer thickness. NMR studies of water adsorbed to porous glass show that 2.5–3 monolayers are essentially in a “frozen” amorphous structure even at room temperature, and that this fraction remains amorphous as the sample is cooled to freezing temperatures [27]. Water confined inside the 2 nm pores of porous glass does not crystallize [28], and it crystallizes only very slowly in the 6.5 nm channels of certain protein crystals [29].

In the context of the glass forming ability of systems including metallic glasses, glassy oxides, and aqueous cryoprotectant solutions, extensive experimental CCR data have been empirically correlated using the parameter

$$\gamma = \frac{T_x}{T_l + T_g}, \quad (10)$$

where T_g is the glass temperature, T_l is the liquidus temperature, and T_x is the devitrification temperature of the solution [7]. While this empirical correlation works well for the systems and concentration ranges from which it was derived, it fails for the less-concentrated cryoprotectant solutions reported here. For example, scaling the measured CCR of a 30% (w/v) glycerol solution requires $T_x = 123$ K, well below $T_g = 148$ K [30].

The nucleation model proposed here makes no assumptions that limit its applicability to aqueous solutions. Equation (7) may thus be expected to hold in arbitrary systems where a favored phase nucleates in the presence of a species that must be excluded from the critical cluster. To test the generality of Eq. (7), we performed lattice simulations of nucleation in an Ising system below the critical temperature in the presence of otherwise noninteracting solutes that were excluded from the nucleating phase by hard-wall interactions. The simulations demonstrate that the free energy of a cluster containing N sites is increased by nNk_bT where n is the volume fraction of solutes, consistent with the third term in Eq. (7). Furthermore, when nearest-neighbor interactions between the nucleating phase and solutes are included, the basic features of the exclusion radius, R_e , are captured.

This work was supported by the NSF (Grants No. DMR-0805240 and No. DMR-1005479) and by the NIH (Grant No. R01 GM65981).

*Corresponding authors.

maw64@cornell.edu

ret6@cornell.edu

- [1] P. Mazur, *Science* **168**, 939 (1970).
- [2] H. Hope, *Acta Crystallogr. Sect. B* **44**, 22 (1988).
- [3] D. W. Rodgers, *Structure* **2**, 1135 (1994).
- [4] D. M. Murphy, *Geophys. Res. Lett.* **30**, 2230 (2003).
- [5] M. B. Baker, *Science* **276**, 1072 (1997).
- [6] P. G. Debenedetti, *J. Phys. Condens. Matter* **15**, R1669 (2003).
- [7] Z. P. Lu and C. T. Liu, *Phys. Rev. Lett.* **91**, 115505 (2003).
- [8] V. Berejnov, N. S. Hussein, O. A. Alsaied, and R. E. Thorne, *J. Appl. Crystallogr.* **39**, 244 (2006).
- [9] M. Warkentin, V. Stanislavskaja, K. Hammes, and R. E. Thorne, *J. Appl. Crystallogr.* **41**, 791 (2008).
- [10] P. Bruggeller and E. Mayer, *Nature (London)* **288**, 569 (1980).
- [11] I. Kohl, L. Bachmann, A. Hallbrucker, E. Mayer, and T. Loerting, *Phys. Chem. Chem. Phys.* **7**, 3210 (2005).
- [12] L. S. Bartell and J. F. Huang, *J. Phys. Chem.* **98**, 7455 (1994).
- [13] J. F. Huang and L. S. Bartell, *J. Phys. Chem.* **99**, 3924 (1995).
- [14] J. M. Hey and D. R. Macfarlane, *Cryobiology* **33**, 205 (1996).
- [15] J. M. Hey and D. R. Macfarlane, *Cryobiology* **37**, 119 (1998).
- [16] A. Manka, H. Pathak, S. Tanimura, J. Wölk, R. Strey, and B. E. Wyslouzil, *Phys. Chem. Chem. Phys.* **14**, 4505 (2012).
- [17] G. P. Johari, *J. Chem. Phys.* **122**, 194504 (2005).
- [18] S. K. Ma, *Statistical Mechanics* (World Scientific, Philadelphia, 1985), 1st ed., Chap. 11.
- [19] P. J. Atzberger and P. R. Kramer, *Phys. Rev. E* **75**, 061125 (2007).
- [20] L. Hao and D. G. Leaist, *J. Chem. Eng. Data* **41**, 210 (1996).
- [21] N. Kimizuka and T. Suzuki, *J. Phys. Chem. B* **111**, 2268 (2007).
- [22] B. Halle and M. Davidovic, *Proc. Natl. Acad. Sci. U.S.A.* **100**, 12135 (2003).
- [23] M. Heyden, E. Bründermann, U. Heugen, G. Niehues, D. M. Leitner, and M. Havenith, *J. Am. Chem. Soc.* **130**, 5773 (2008).
- [24] R. Kumar, J. R. Schmidt, and J. L. Skinner, *J. Chem. Phys.* **126**, 204107 (2007).
- [25] S. L. Lee, P. G. Debenedetti, and J. R. Errington, *J. Chem. Phys.* **122**, 204511 (2005).
- [26] D. E. Moilanen, E. E. Fenn, D. Wong, and M. D. Fayer, *J. Chem. Phys.* **131**, 014704 (2009).
- [27] K. Overloop and L. Vangerven, *J. Magn. Reson., Ser. A* **101**, 179 (1993).
- [28] J. Rault, R. Neffati, and P. Judeinstein, *Eur. Phys. J. B* **36**, 627 (2003).
- [29] M. Weik, G. Kryger, A. M. M. Schreurs, B. Bouma, I. Silman, J. L. Sussman, P. Gros, and J. Kroon, *Acta Crystallogr. Sect. D* **57**, 566 (2001).
- [30] D. Harran, *Bull. Soc. Chim. Fr.* **1–2**, 140 (1978).